Science of the Total Environment 788 (2021) 147914

Contents lists available at ScienceDirect

Science of the Total Environment

journal homepage: www.elsevier.com/locate/scitotenv

Simulating spatial change of mangrove habitat under the impact of coastal land use: Coupling MaxEnt and Dyna-CLUE models

Yuyu Wang [a,1], Bixiao Chao [a,b,1], Peng Dong [c], Dian Zhang [b], Weiwei Yu [b,d], Wenjia Hu [b,d,*], Zhiyuan Ma [b,d], Guangcheng Chen [b,d], Zhenghua Liu [b], Bin Chen [b,d,*]

[a] School of Ecology and Nature Conservation, Beijing Forestry University, Beijing 100083, PR China
[b] Third Institute of Oceanography, Ministry of Natural Resources, Xiamen 361005, PR China
[c] Aerospace Information Research Institute, Chinese Academy of Sciences, Beijing 100094, PR China
[d] Fujian Provincial Key Laboratory of Marine Ecological Conservation and Restoration, Xiamen 361005, PR China

HIGHLIGHTS

- We predicted mangrove habitat changes in Guangdong, China considering land-use change.
- Species distribution and land-use models were coupled as an integrated framework.
- Under the current trend, only 70% of the mangrove habitats would remain in 2030.
- Potential mangrove habitats would increase by 11%–61% with improved land-use policies.

GRAPHICAL ABSTRACT

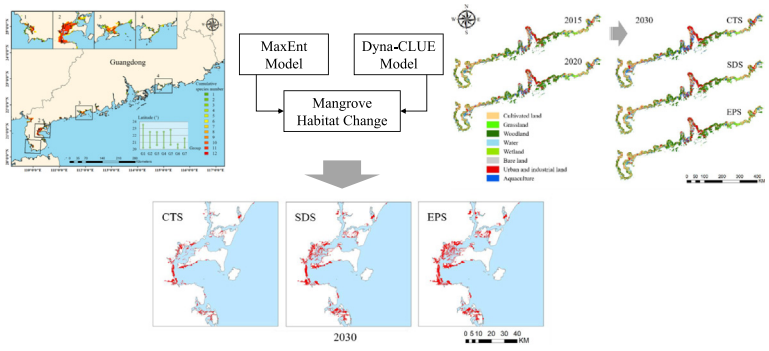

ARTICLE INFO

Article history:
Received 16 March 2021
Received in revised form 15 May 2021
Accepted 15 May 2021
Available online 21 May 2021

Editor: Fernando A.L. Pacheco

Keywords:
Restoration potential
Policy scenario
Guangdong Province
Mangrove afforestation
Conservation strategy

ABSTRACT

Global mangrove forests have exhibited distinct changes in the past decades owing to anthropogenic activities, with land-use pressure being among the main causes of mangrove loss. Thus, understanding the inherent conflicts between conservation/restoration and land-use demands is fundamental for mangrove management. To predict how land-use changes will drive the spatiotemporal patterns of mangrove habitats, a novel integrated framework coupling MaxEnt and Dyna-CLUE modeling was proposed. The coupled model can identify suitable mangrove afforestation habitats and predict the impact of land-use change on potential mangrove habitats. In this study, the model was used to predict the mangrove habitat change in 2030 in the province with the most mangrove forests in China. The potential suitable habitat of 14 mangrove species under three coastal land-use scenarios were mapped using the coupled model. Under the current trend scenario, only 41.2% of the existing wetland would be retained, whereas the potential distribution area of all the mangrove species will decrease by an average of 30%. Under the sustainable development and ecological protection scenarios, the mangrove habitat could be increased by 11% to 61%, depending on the species. Different mangrove species showed varied sensitivity to the improved land-use policies, with several species being harder to restore than others, even under aggressive protection and restoration policies. The combined use of both MaxEnt and Dyna-CLUE models proved complementary and offered insights into the impacts of different land-use policies on the spatiotemporal change of mangrove habitats.

* Corresponding authors at: Third Institute of Oceanography, Ministry of Natural Resources, Xiamen 361005, PR China.
E-mail addresses: huwenjia@tio.org.cn (W. Hu), chenbin@tio.org.cn (B. Chen).
[1] These authors contributed equally to this work and should be considered co-first authors.

https://doi.org/10.1016/j.scitotenv.2021.147914
0048-9697/

1. Introduction

Mangrove ecosystems are distributed along the coasts in tropical and subtropical regions between latitudes of approximately 30° N and 30° S (Giri et al., 2011) and provide valuable ecosystem services by supporting coastal fisheries (Zhang et al., 2019) while yielding commercial forest products (Blasco et al., 1996). They also provide coastal protection by regulating flooding, erosion, siltation, and tidal surges (Alongi, 2008; Giri et al., 2011), while storing and sequestering relatively large quantities of carbon (Sasmito et al., 2019). Additionally, millions of coastal residents live around mangrove ecosystems and draw heavily from their goods and services (Atkinson et al., 2016; Gevana et al., 2015).

The proximity of mangroves to coastal population centers leads to massive degradation and loss. In the last two decades of the 20th century, approximately 35% of mangroves disappeared (Valiela et al., 2001), with only 15.2 million hectares of mangroves remaining worldwide (Spalding et al., 2010). Furthermore, mangroves are on the verge of extinction in 26 out of the 120 countries with mangroves (FAO, 2007), owing to land use and land cover (LULC) changes from small-scale tree harvesting for firewood (Malik et al., 2017) to industrial-scale logging for timber (Sillanpaa et al., 2017) and clear-cutting for aquaculture ponds (Richards and Friess, 2016; Thomas et al., 2017; Jia et al., 2018) that replaced mangrove areas worldwide. In addition, mangrove clearance for urban expansion and development of coastal infrastructure has added to the losses, particularly in places where coastal populations are rapidly expanding (Worthington and Spalding, 2018). For example, a massive loss of mangrove forests, approximately 1.9 million hectares, has been reported in Asia since 1980 (Malik et al., 2017).

In China, a total of 12,924 ha of mangrove forests have disappeared between 1980 and 2000 (Jia et al., 2018). Reclamation was the main cause of mangrove forest loss, with 97.6% being used to build aquaculture ponds (Paulson Institute, 2020). The increase in urban construction land and decrease in mangrove forests also showed a significant correlation (Tuholskea et al., 2017). In recent years, mangrove conservation and restoration efforts in China have faced problems, such as insufficient effectiveness and low survival rates (Peng et al., 2016). The reasons for this include urbanization and reclamation of suitable mangrove habitats and improper site selection of restoration projects (Fan and Wang, 2017; Jia et al., 2018), with only 57% of the replanted mangroves being successfully restored nationwide (Chen et al., 2009). In the National Action Plan for Mangrove Conservation and Restoration (2020–2025), the Chinese government planned to restore 18,800 ha of mangroves by 2025 (MNR and NFGA, 2020). Moreover, it is now acknowledged that improved mangrove ecosystem management, by preventing further land-use change and promoting regeneration efforts, i.e., restoration, rehabilitation, and afforestation, is fundamental for mangrove conservation (Peng et al., 2016; Jia et al., 2018; Sasmito et al., 2019). Thus, balancing the economic growth needs of land and mangrove habitat conservation/restoration is a significant challenge, and knowledge on the spatial distribution of mangrove habitat changes driven by land-use pressure, the change rates, and the effect of different policies can provide an important scientific basis for the formulation of management strategies.

Ideally, mangroves can be afforested in theoretically suitable areas. However, owing to coastal socioeconomic development, not all of these areas are available for mangrove afforestation, such as urban and aquaculture areas. Several tools can be used to assess this issue. Suitable habitats for mangroves can be mapped using species distribution models (SDMs) (Johnson et al., 2006; Phillips et al., 2017). SDMs can analyze the relationship between species distribution data and environmental factors through statistical algorithms to predict the distribution probability of related species (Kulhanek et al., 2011; Li et al., 2019), and have been successfully used to map suitable areas of mangroves (Charrua et al., 2020; Hu et al., 2020a), with the maximum entropy model (MaxEnt) showing the best performance. On the other hand, land-use change models are often used to simulate land-use dynamics and support political decisions on land-use management (Tesfaw et al., 2018; Peng et al., 2020). Land-use change models can determine where (location of change) and at what rate land-use changes are likely to occur (quantity of change) (Trisurat et al., 2010; Sakayarote and Shrestha, 2019). However, these two model types are usually used independently, i.e., either considering natural suitability (Charrua et al., 2020; Hu et al., 2020b) or land-use pressures (Sardar and Samadder, 2021), and have seldom been combined to study the spatiotemporal dynamics of mangrove habitats. Coupling SDMs and land-use change models can address how suitable habitats for mangroves interact with future land-use changes and help make suggestions for appropriate land-use and mangrove management policies.

To predict the conflict between mangrove habitat and land use, and explore how land-use changes will drive the spatiotemporal patterns of mangrove habitats, this study combined an SDM and land-use change model focusing on Guangdong Province. Guangdong has the largest mangrove distribution area among China's coastal provinces (Dan et al., 2016), and is the most economically developed coastal regions in the nation, facing huge development pressures. We aimed to (1) develop an integrated framework to assess mangrove habitat dynamics under land-use pressures across space and time; (2) identify suitable afforestation habitats for different mangrove species; (3) simulate land-use and mangrove potential habitat changes until 2030 under three policy scenarios; and (4) evaluate the impacts of different land-use policies to provide information for mangrove protection and restoration management.

2. Methods

2.1. Study area

Guangdong Province is located at 20° 13′ N –25° 31′ N and 109° 39′ E −117° 19′ E, with the Tropic of Cancer running through the province (Liao and Zhang, 2014), and its coastline (8500 km) covers the northern tropical and southern subtropical temperature zones. The Gross Domestic Product (GDP) of Guangdong ranks first nationwide with over 115 million people (NBSC, 2020), and its GDP growth rate was 6.2% in 2019, making it one of the fastest economically growing regions worldwide (Lv et al., 2012). According to the Second National Wetland Resources Survey, 57.3% of China's mangroves are scattered along the coastline of Guangdong (Fig. 1), with an area of 12,040 ha (Dan et al., 2016; Yang et al., 2018; Wu et al., 2011). There are 14 native true mangrove species, with *Avicennia marina*, *Aegiceras corniculatum*, *Sonneratia caseolaris*, and *Kandelia obovata* being the most common species (Yang et al., 2018).

2.2. Methodology framework

An integrated framework was proposed to identify suitable mangrove afforestation habitats and predict the impact of future land-use change on mangrove habitats based on MaxEnt and Dyna-CLUE modeling (Fig. 2). The proposed approach consists of four steps: (1) dataset collection and processing, including mangrove presence, environmental, LULC, and socioeconomic data; (2) predicting the potential suitability of mangrove distribution by MaxEnt modeling using the presence data and environmental variables; (3) simulating the 2030 land-use change under three scenarios through Dyna-CLUE modeling; (4) predicting the spatial change of mangrove habitat under the constraints of land-use pattern by deducting all the artificial land-use types from the theoretically suitable area of mangroves (Bastin et al., 2019; Vessella and Schirone, 2013).

2.3. MaxEnt modeling

2.3.1. Species occurrence records

ESRI World Imagery 2018 (resolution 2.5 m) was used to visually interpret the mangrove forest patches along the coast. The patches in

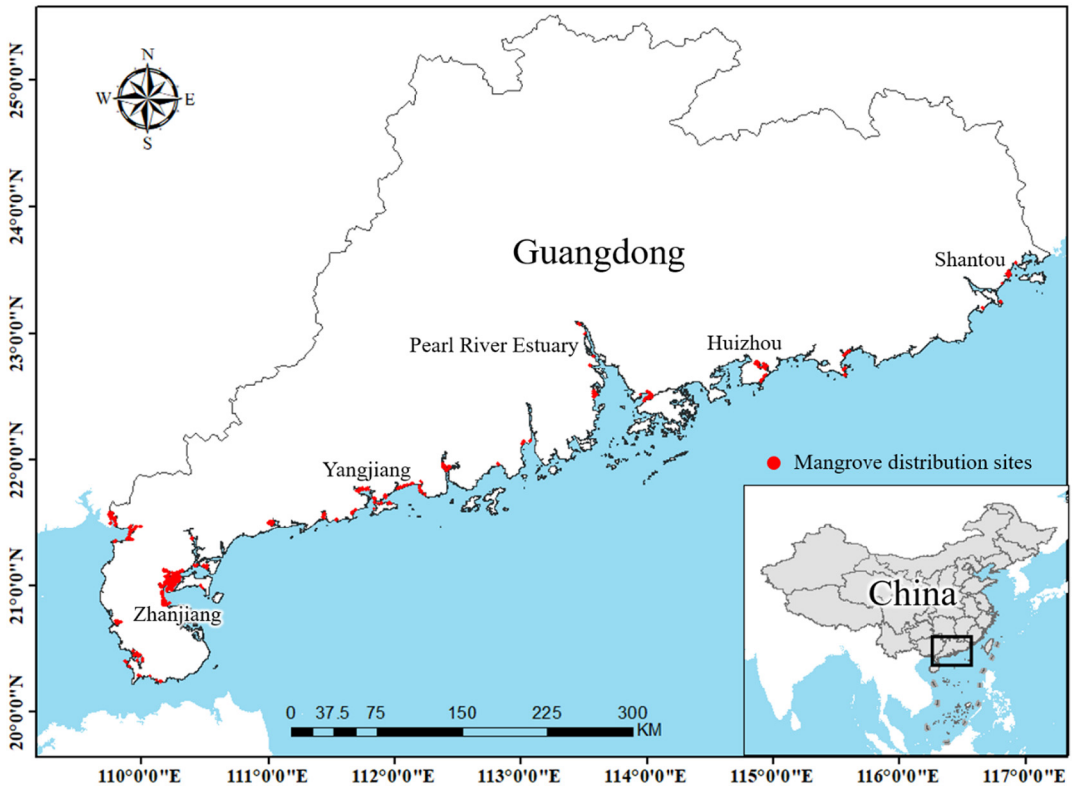

Fig. 1. Study area and mangrove occurrence records.

Zhanjiang, the Pearl River Estuary, and Shantou were then checked through on-site investigations in 2018–2019. Reconnaissance and sampling surveys were conducted and combined with historical records from the literature review (Chen et al., 2017; Li et al., 2016; Lin et al., 2006) to determine the distribution of mangrove species. Thereafter, 196 patches (Fig. 1) were resampled into points using the Fishnet method in ArcGIS Pro 2.6.2, with a sampling resolution of 100 m. Finally, 7777 occurrence points were obtained to generate the species presence dataset. As these mangroves comprised temperature-limited species (Lin and Fu, 1995; Wu et al., 2018), we divided the 14 species into seven groups according to their distribution margin and cold tolerance (Table 1). According to the occurrence of each group, the sampling

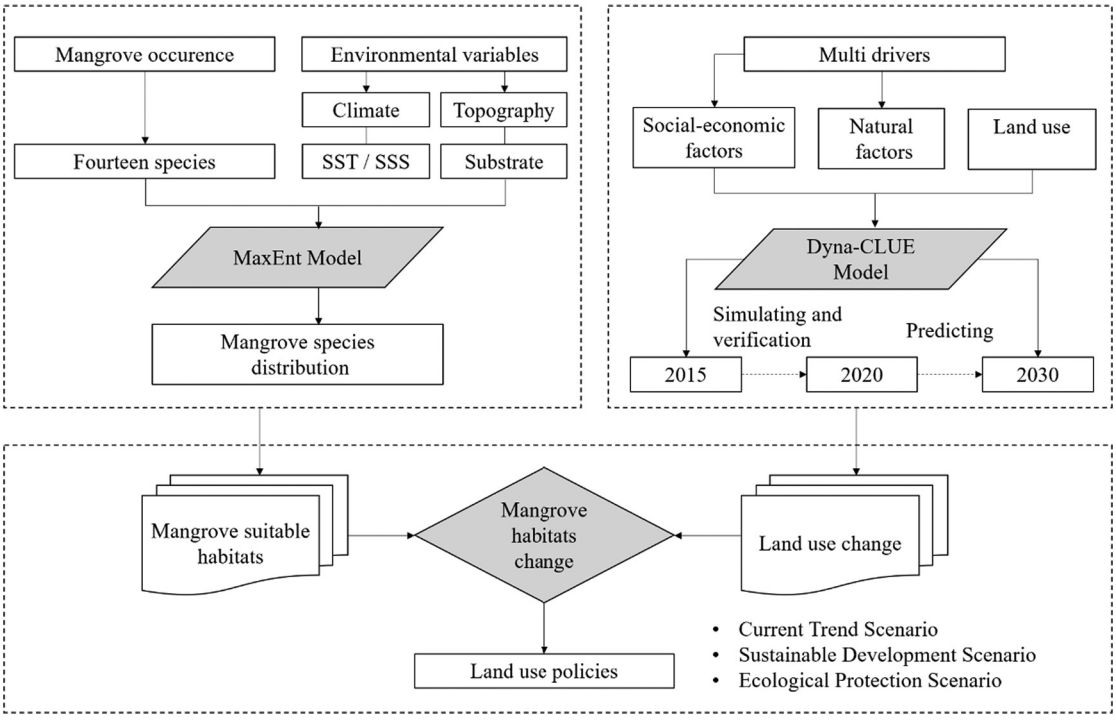

Fig. 2. Methodological framework. SSS, sea surface salinity; SST, sea surface temperature.

Table 1
Groups and distribution of native mangrove species in Guangdong Province, China.

Group	Species	Distribution sites (listed by prefecture-level city, from south to north)										
		South Zhanjiang	North Zhanjiang	Maoming	Yangjiang	Jiangmen	Zhongshan	Guangzhou	Shenzhen	Huizhou	Shanwei	Shantou
G1	*Kandelia obovata, Aegiceras corniculatum, Avicennia marina, Acanthus ilicifolius, Bruguiera gymnorhiza, Excoecaria agallocha*	+	+	+	+	+	+	+	+	+	+	+
G2	*Rhizophora stylosa*	+	+	+	+	+	+					
G3	*Ceriops tagal*		+	+	+	+	+					
G4	*Acrostichum aureum*	+	+	+	+	+	+		+			
G5	*Lumnitzera racemosa*		+	+	+	+	+			+		
G6	*Acrostichum speciosum, Acanthus ebracteatus, Bruguiera sexangula*	+										
G7	*Sonneratia caseolaris*	+	+									

points were allocated to the corresponding area to generate the presence data for each group.

2.3.2. Environmental variables

Temperature, salinity, substrate, and distance from the coastline are important factors affecting the growth and distribution of mangroves (Peng et al., 2016). In this study, the original environmental dataset contained 40 variables related to mangrove distribution, including bioclimatic, terrain, substrate, sea surface temperature (SST), and sea surface salinity (SSS) variables. As strong variable collinearity may cause misinterpretation of the MaxEnt model owing to the high correlation level among variables (Jayasinghe and Kumara, 2019), a correlation analysis of 40 environmental variables was performed. The variables with high correlation (Pearson correlation coefficient $|r| \geq 0.8$) were removed, and the less correlated variables were retained for the MaxEnt model (Chakraborty et al., 2016; Wei et al., 2018; Jayasinghe and Kumara, 2019). The resultant variable set contained 20 predictors (Table 2). All the environmental variable layers were interpolated into the coastal area with a 10 km buffer zone along the coastline and standardized into the same 1 km grids. Finally, these layers were converted to ASCII format for further processing in MaxEnt.

2.3.3. Model settings and evaluation

Suitable habitats for mangroves in Guangdong Province were predicted using MaxEnt 3.4.1 (Phillips et al., 2017). MaxEnt estimates the habitat suitability of targeted species by finding the maximum entropy of the species distribution based on input presence data and environmental variables (Phillips et al., 2006). In the present study, 75% of the presence data was randomly selected as training data, while the remaining 25% was used as testing data. The recommended default parameters for the convergence threshold (10–5), maximum number of iterations (500), maximum number of background points (10,000), and bootstrap resampling method were used. The averaged result from 10 replications was taken as the final output.

Model performance was evaluated based on the area under the curve (AUC) of the receiver operating characteristic (ROC) curve. The AUC was used to evaluate the model efficacy, with an AUC closer to 1 indicating better performance (Wang et al., 2020a). The permutation importance of the variables was evaluated using the model and determined by randomly permuting the values of each variable among the training points and measuring the resulting decrease in the training AUC.

2.4. Dyna-CLUE model simulation

2.4.1. Model process and data

The Dyna-CLUE model can simulate and predict the spatial layout of land use through quantitative analysis and summarization of the interactions among different land covers, and natural, policy, and social factors (Verburg and Overmars, 2009). The model includes two parts: a non-spatial demand module for predicting future land use demand and a space allocation module for calculating land use plans. The Dyna-CLUE model calculates the distribution probability of a certain LULC type in a certain area through the spatial module. Then multiple iterations in the non-spatial module are performed according to the initial land use data, land use scenarios, time series, and other parameters, and finally the land use pattern of the forecast year is calculated and determined through the iteration result (Peng et al., 2020).

The change rate of each LULC type was calculated using LULC data for 2015 and 2020 (http://www.resdc.cn/). In the intertidal zone, the distribution dataset of the national wetland and coastal aquaculture ponds (http://gre.geodata.cn) was used to complete the coastal LULC map. Thus, the final map was reclassified into eight LULC types: cultivated land, grassland, woodland, water, wetland, bare land, urban and industrial land, and aquaculture.

Land-use changes are related to various biophysical and socioeconomic drivers (Peng et al., 2020). Thus, five topographic and five socioeconomic indices were input into the model as driving factors (Table 3). Considering the prediction accuracy and operation limit of the Dyna-CLUE model, all data were resampled to 250 m (Gong et al., 2018).

2.4.2. Setting of land-use scenarios

Three scenarios were developed for 2030 according to the current land-use change from 2015 to 2020. The current trend scenario (CTS) was based on the assumption that the tendency of land-use change in the past five years was maintained. The sustainable development scenario (SDS) considered the maintenance and restoration of natural ecosystems while promoting urbanization and economic development. Aquaculture was the main reason for the destruction of mangroves (Fan and Wang, 2017; Paulson Institute, 2020), and due to unsustainable aquaculture development, approximately 30% of aquaculture ponds are currently abandoned and unused (Paulson Institute, 2020). Based on these data, in SDS, the change rate of artificial land types was assumed to be reduced by 50%, whereas 50% of the aquaculture area located at 0–6 m water depth would be restored to wetland. The ecological protection scenario (EPS) considered aggressive ecological protection and restoration policy, completely stopping the transfer from natural to artificial land types. In this scenario, the urban and industrial land was assumed to stop expanding. The decreasing trend of natural land types was assumed to be reversed, the increasing trend would be half of the historical decreasing rate. Moreover, 100% of the aquaculture area located at a water depth of 0–6 m would be restored to wetlands. The spatial land-use changes of these scenarios were simulated with the Dyna-CLUE model (version 2.0) (Verburg et al., 2002; Overmars et al., 2007) based on the 10 driving factors.

2.4.3. Model evaluation

The fitness of driving factors and land conversion were tested using the ROC method (Swets, 1988; Pontius et al., 2008). Model accuracy was

Table 2
List of environment variables used in MaxEnt modeling.

Data types	Environmental variables	Units	Data sources
Bioclimatic	Annual mean temperature	°C	WorldClim version 2.1 (www.worldclim.org)
	Mean diurnal range	°C	
	Isothermality	%	
	Range of annual temperature variation	°C	
	Mean temperature of wettest quarter	°C	
	Annual precipitation	mm	
	Precipitation seasonality	%	
	Precipitation of warmest quarter	mm	
	Precipitation of coldest quarter	mm	
Topographic	Euclidean distance to the coast	M	The Pacific Islands Ocean Observing System's Distance to Nearest Coastline (http://oos.soest.hawaii.edu/thredds/ncss/dist2coast_1deg_ocean/dataset.html)
	Compound Topographic Index	–	Calculated by ArcGIS Pro 2.6.2 according to elevation data
	Elevation	–	ETOPO1 bathymetry data from NOAA https://www.ngdc.noaa.gov/mgg/global/global.html
	Local deviation from global	–	Calculated by ArcGIS Pro 2.6.2 according to elevation data
Substrate	Substrate type	–	2018 AHO S57 map
Sea surface salinity (SSS)	Annual SSS mean	‰	Bio-ORACLE dataset (www.bio-oracle.org)
	Annual SSS range	‰	
Sea surface temperature (SST)	Mean SST of coldest quarter	°C	Derived from NASA MODIS-Aqua Level-3(http://oceancolor.gsfc.nasa.gov)
	Monthly SST range		
	Annual SST mean		
	Annual SST range		

assessed using the kappa value, which compared the predicted result with the actual LULC pattern in 2020 (Peng et al., 2020).

$$Kappa = (P_0 - P_c)/(P_p - P_c),$$

where P_0 is the proportion of correct simulation, i.e., the consistency ratio between the real and simulation images; P_c is the expected correct simulation ratio under random conditions, calculated from the transition matrix of the simulated land-use map and the actual land-use map; and P_p is the correct simulation ratio under the ideal classification condition, which is generally assigned as 1 (Wischmeier and Smith, 1978). If the two phases of land-use type maps are identical, the kappa value is 1, whereas if the kappa value is less than 0.4, the simulation effect is considered poor (Liao et al., 2019).

2.5. Habitat change calculation

First, for each species group, a binary map was generated based on habitat suitability, with a suitability threshold of 0.5 (Wang et al., 2020b). Grids with a value of 1 indicated that the area was a potential habitat for mangroves, meanwhile grids with a value of 0 were considered to have inadequate environmental conditions for mangrove growth. Then, the artificial land types (cultivated land, urban and industrial land, and aquaculture) in current and future scenarios were regarded as areas that were not available for afforestation and were excluded from the binary maps. The potential restorable habitats were finally identified by deducting the artificial lands and unsuitable habitats, and the changes in trends were analyzed based on these results.

3. Results

3.1. Theoretical distribution of mangrove habitats

In the MaxEnt modeling, the averaged AUC values of the seven species groups were between 0.89 and 0.99, indicating that the model performed well in identifying the mangrove habitat distribution. Furthermore, the potential distribution ranges varied significantly among groups. G1 and G6 had the widest and narrowest distribution, with an area of 160,513 and 9663 ha, respectively. Stacking the distributions of all groups, species richness decreased with increasing latitude (Fig. 3), and the predicted suitable range for most mangrove species was between 20.5° N and 22.5° N.

By analyzing the environmental variable permutation importance, we found that the importance of environmental drivers also varied among groups. Nevertheless, variables from types of precipitation, salinity, and sea surface temperature mostly determined the distribution of mangroves in Guangdong Province. We screened and listed the top three important variables for each group in Table 4. The annual precipitation, SST in the coldest season, and salinity range showed important contributions in most groups. These environmental variables were used to describe the multidimensional niche of each group (Fig. 4), and indicated that the niches for G1 and G4 were wider than those of other groups, whereas the niches for G6 and G7 were the narrowest,

Table 3
Driving factors used in Dyna-CLUE modeling.

Data types	Driving factors	Units	Data sources
Topographic	Elevation	m	National Catalogue Service for Geographic Information (http://mulu.tianditu.gov.cn/)
	Slope	°	
	Aspect	–	
	Soil erosion	–	Resource and Environment Science and Data Center (http://www.resdc.cn/)
	Soil texture	–	
Socioeconomic	Distance to rivers	m	National Catalogue Service for Geographic Information (http://mulu.tianditu.gov.cn/)
	Distance to roads	m	
	Distance to settlements	m	
	GDP	Yuan $km^2\ y^{-1}$	Resource and Environment Science and Data Center (http://www.resdc.cn/)
	Population	Person $km^{-2}\ y^{-1}$	

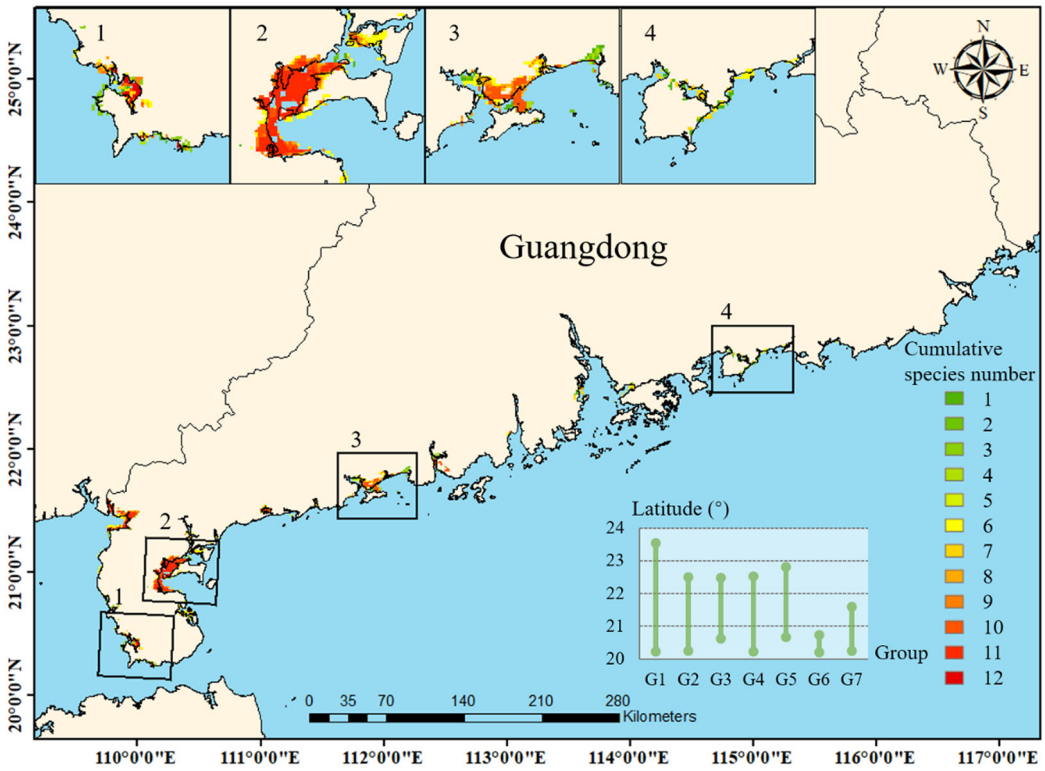

Fig. 3. Suitable habitat distribution of 14 mangrove species in Guangdong Province. 1, southwest coast of Zhanjiang; 2, east coast of Zhanjiang; 3, Yangjiang; 4, Huizhou.

preferring an environment with stable salinity and relatively less precipitation.

3.2. Land-use change prediction

The AUC values for the Dyna-CLUE predictions were 0.54–0.84, 88% of which exceeded 0.70 (Table 5), indicating that the selected driving factors had strong explanatory power for the conversion of land-use types. Moreover, the kappa value for the 2020 simulated and actual land-use was 0.54, which suggested that the model had reliable prediction ability.

The coastal zone of Guangdong is a typical area with rapid socioeconomic development and urbanization. Under CTS, aquaculture and urban/industrial land were the main net inflow land types, and the natural land types were mainly outflow. However, under the alternative land-use policies, land-use transfer patterns showed great changes. For example, under SDS, the urbanization process would take up a large amount of cultivated land, whereas cultivated land and aquacultural areas would be returned to natural land types. Under EPS, a large number of aquacultural areas would be restored to wetlands, whereas the cultivated areas would be returned to grassland, woodland, and water (Fig. 5).

Currently, the scattered mangrove patches are mainly distributed as wetlands, water, and woodland. Under CTS, these land-use types were all reduced, especially the wetland, with a decline so fast that, at this rate, only 41.2% of the existing wetlands would remain by 2030 (Table 6). Under SDS, the woodland and water areas were maintained at the level they were in 2020, and the area of wetland increased significantly. Meanwhile, under EPS, woodland and water areas were restored to those of 2015, and the wetland area was restored to over three times that in 2015 (Fig. 6).

Table 4
Permutation on importance of environmental variables.

Environmental variable	G1	G2	G3	G4	G5	G6	G7
Annual precipitation	6.4	14.5	14.5	14.5	15.6	23.4	20.7
Precipitation seasonality	1.7	2.4	0.9	2	0.1	1.3	13.7
Precipitation of warmest quarter	12.6	3.4	2.4	1.6	11	0	4.1
Precipitation of coldest quarter	1.6	10.2	11.9	16.1	9.2	3.2	0.2
Annual SSS mean	0.8	3.1	3.7	1.6	3.4	52.6	0
Annual SSS range	9.5	13.4	17.3	7.5	15.6	0.6	34.4
Annual SST mean	7.3	15.5	7.8	3.6	7.2	4.8	6
Annual SST range	9.9	2	1.6	3.4	1.8	0	2.6
Mean SST of the coldest quarter	5.6	12.1	12.1	15.6	11.1	0.5	2.4

Note: Gray background indicates the top three important variables for each species group.

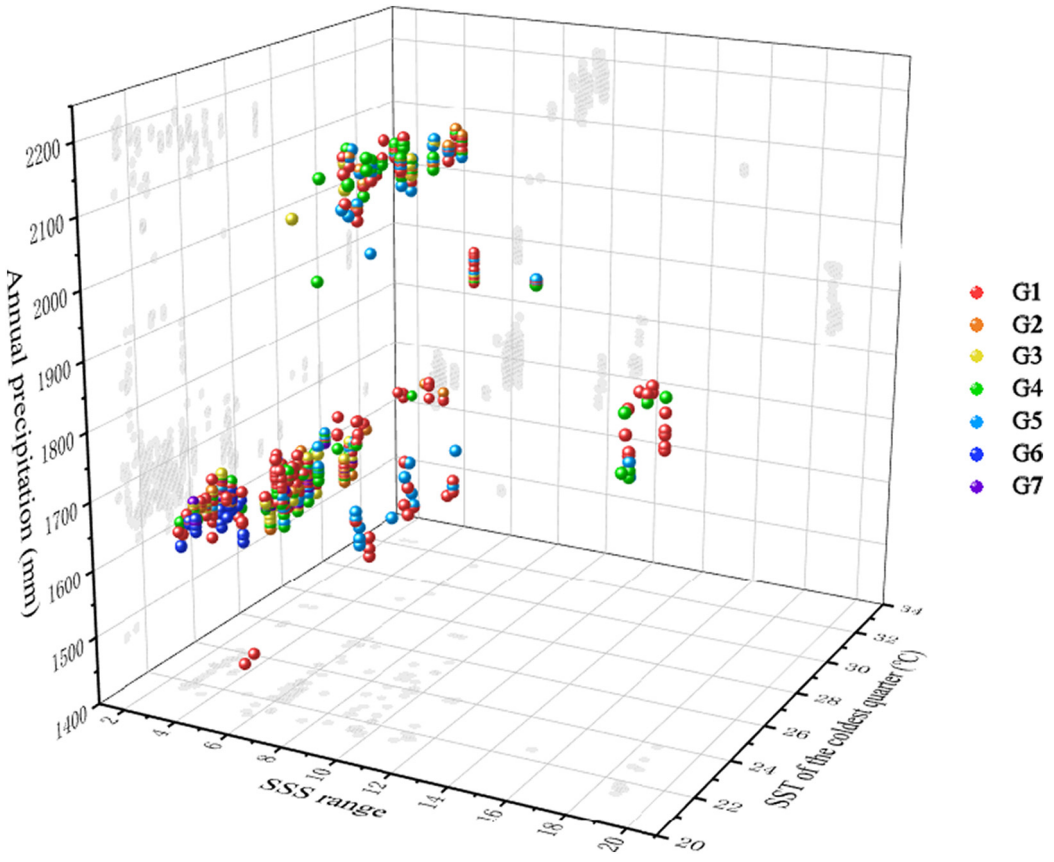

Fig. 4. Ecological niches of seven species groups.

3.3. The impacts of land-use change on mangrove habitats

The suitable areas estimated using MaxEnt described the environmental limits for the presence of mangrove species. Next, the current and future anthropogenic factors (urbanization, restoration, etc.) were imposed onto the theoretically suitable areas to predict the actual afforestation extent of mangrove forests (Table 7). All artificial land types (cultivated land, urban and industrial land, and aquaculture) were deducted from the theoretically suitable mangrove areas, with G1 and G6 showing the largest and smallest distribution range, respectively, under all current and future scenarios. Driven by the simulated land-use pattern in 2030, the actual available habitat ranges of all groups were predicted to decline significantly under CTS, with an obvious fragmentation of the mangrove forest patches. In contrast, the mangrove distribution range increased significantly under SDS and EPS, maintaining and promoting the integrity of habitat patches (Fig. 7).

Table 5
AUC values of each land-use type fitted by using the Dyna-CLUE model.

Land-use types	AUC	
	2015–2020	2020–2030
Cultivated land	0.70	0.69
Grassland	0.73	0.74
Woodland	0.83	0.84
Water	0.75	0.79
Wetland	0.81	0.79
Bare land	0.80	0.73
Urban and industrial land	0.78	0.79
Aquaculture	0.84	0.84

According to the results, if the current land-use policy is maintained until 2030, the potential distribution area of all mangrove species will decrease by an average of approximately 30%. However, under the other two scenarios, different mangrove species showed varied sensitivity to conservation and restoration policies. The mangrove distribution area could be increased by 11%–61% depending on the different scenarios and species groups. Among all groups, G6 showed the least optimistic scenario, with difficulties to achieve effective growth even under aggressive protection and restoration scenarios (Fig. 8).

4. Discussion

4.1. Mangrove conservation and restoration implications

Our study estimated the potential suitable habitat of 14 mangrove species in the Guangdong Province. According to the Red List of Threatened Species of China, *A. speciosum* and *A. ebracteatus* in G6 are classified as endangered, whereas *B. sexangula* and *S. caseolaris* in G6 and G7, respectively, are classified as near-threatened (Wang et al., 2020b). These two groups also showed the narrowest distribution ranges and ecological niches according to the modeled results, which may be related to physiological characteristics (Chen et al., 2010). For example, *A. ebracteatus* has a poor tolerance to water and strong light, and only grows in the inner edge of mangrove forests, with a restricted distribution, mostly in the upper intertidal zones (Huang et al., 2020). Meanwhile, their limited environmental adaptability makes them more susceptible to external pressures, accelerating their degradation. For instance, aquaculture development was the most important reason for the loss of *A. speciosum*, *B. sexangula,* and *S. caseolaris* in their original distribution sites in the 1990s (Mao, 2011). Therefore, we recommend that these species should be protected as a priority, not only by

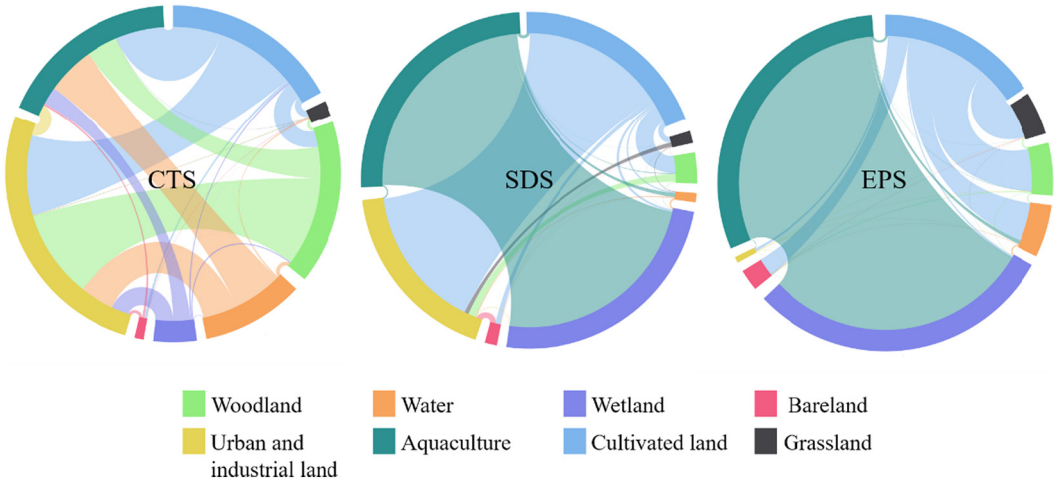

Fig. 5. Coastal zone land-use transfer relationships under three 2030 scenarios. CTS, current trend scenario; SDS, sustainable development scenario; EPS, ecological protection scenario.

Table 6
Areas of land use and land cover types in 2015, 2020, and three scenarios of 2030 (ha).

Land-use type	2015	2020	2030		
			CTS	SDS	EPS
Cultivated land	920,856	896,788	836,770	850,521	836,770
Grassland	118,625	121,869	126,756	122,046	139,392
Woodland	907,063	892,319	849,866	893,616	907,025
Water	240,756	221,919	185,147	222,241	240,518
Wetland	41,206	26,938	11,099	86,784	146,631
Bare land	10,694	10,175	9056	10,190	19,363
Urban and industrial land	384,375	424,425	510,971	468,880	424,425
Aquaculture	247,125	276,269	341,035	216,422	156,575
Total	2,870,700	2,870,700	2,870,700	2,870,700	2,870,700

protecting their natural forests, but also by removing stress from human activities.

The mangrove species richness in Guangdong Province decreases with increasing latitude (Quisthoudt et al., 2012; Wu et al., 2018). Species in G1 can be promoted in the whole region as alternative afforestation species, followed by G2 to G5. In contrast, G6 and G7 species were distributed in a narrow niche and only suitable for the southernmost part of the study area. Latitude limitation suggests that owing to tolerance to low temperatures, the success rate of restoration may be reduced by transplanting species in G6 northward. In the Pearl River Estuary, most of the introduced species of G6 died after the extremely cold winter of 2008, whereas the native species *K. obovata*, *A. corniculatum*, and *A. marina* (G1) survived (Chen et al., 2012). In Shantou, after years of afforestation practice, most of the existing mangrove species belong to G1 (Peng et al., 2015).

Furthermore, our results support site selection for mangrove conservation and restoration. Areas with the richest mangrove species, such as east Zhanjiang and Yangjiang, where 12 species could coexist, should be considered a conservation priority to improve the effectiveness of protection. In addition, the MaxEnt model errors of commission, i.e., regions with high habitat suitability where the species is not currently present, can be considered as candidate sites for mangrove restoration (Bittner et al., 2020).

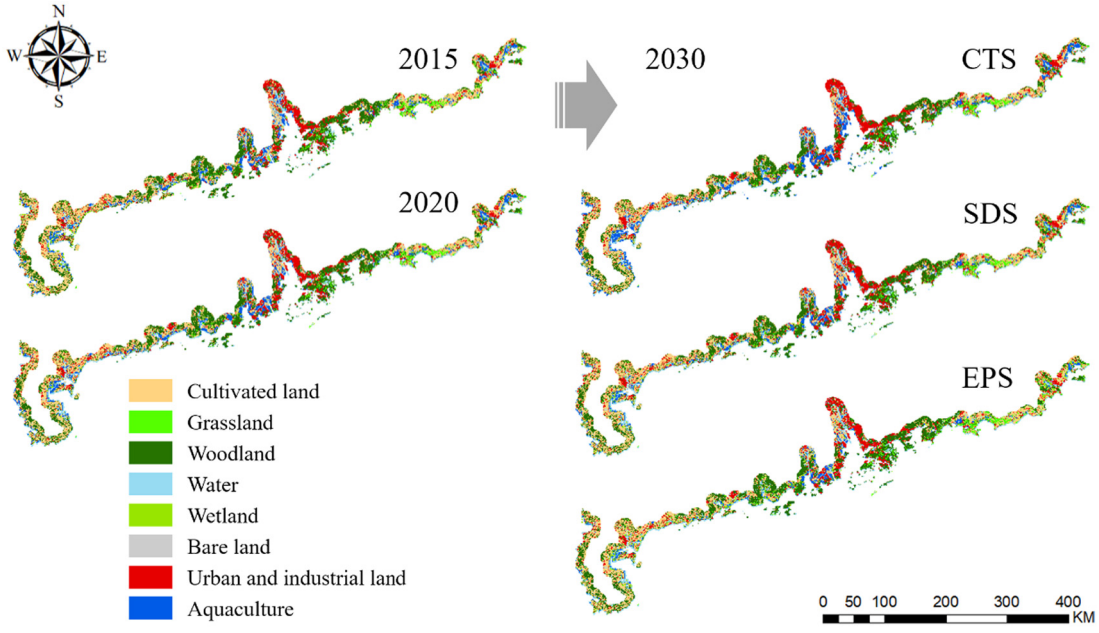

Fig. 6. Land-use pattern in 2015, 2020, and 2030 under three scenarios. CTS, current trend scenario; SDS, sustainable development scenario; EPS, ecological protection scenario.

Table 7
Deducted results under different land-use scenarios, indicating the available areas for mangrove forests (ha).

Group	2020	CTS	SDS	EPS
G1	34,531	24,263	41,575	52,138
G2	22,275	15,694	27,406	34,950
G3	20,088	13,950	24,713	31,525
G4	24,981	16,881	29,900	37,969
G5	21,731	15,588	27,200	34,906
G6	2038	1613	2269	2538
G7	11,713	7831	13,219	15,494

4.2. Drivers of mangrove habitat change and the effect of land-use policies

Simulation of land-use from 2020 to 2030 under the three scenarios demonstrated that land-use change was the crucial driver of mangrove habitat shrinkage. Under CTS, the continuous expansion of aquaculture, as well as urban and industrial land, led to a significant decrease in mangrove habitat. We found that the existing mangrove patches are close to the edge of aquaculture ponds and thus easily affected by aquaculture activities, resulting in habitat degradation or direct occupation by aquaculture activities. Research on the impact of aquaculture ponds on

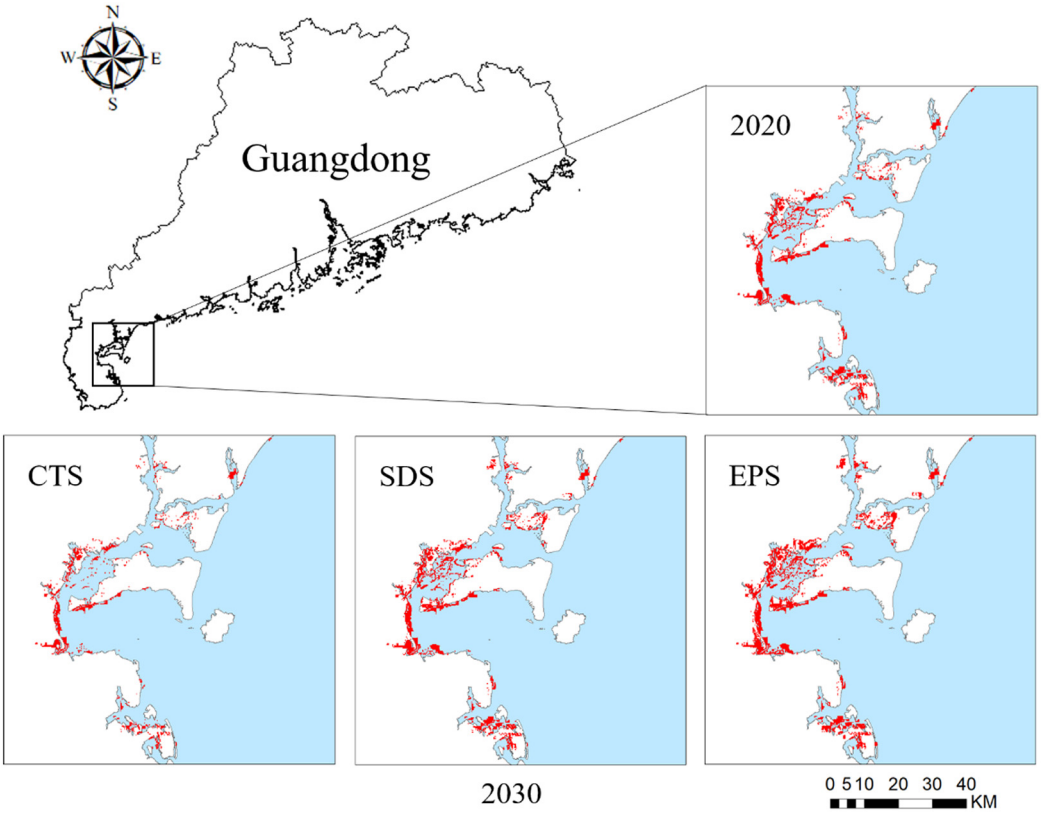

Fig. 7. Changes in mangrove habitat patches under different land-use scenarios, taking G1 as an example. CTS, current trend scenario; SDS, sustainable development scenario; EPS, ecological protection scenario.

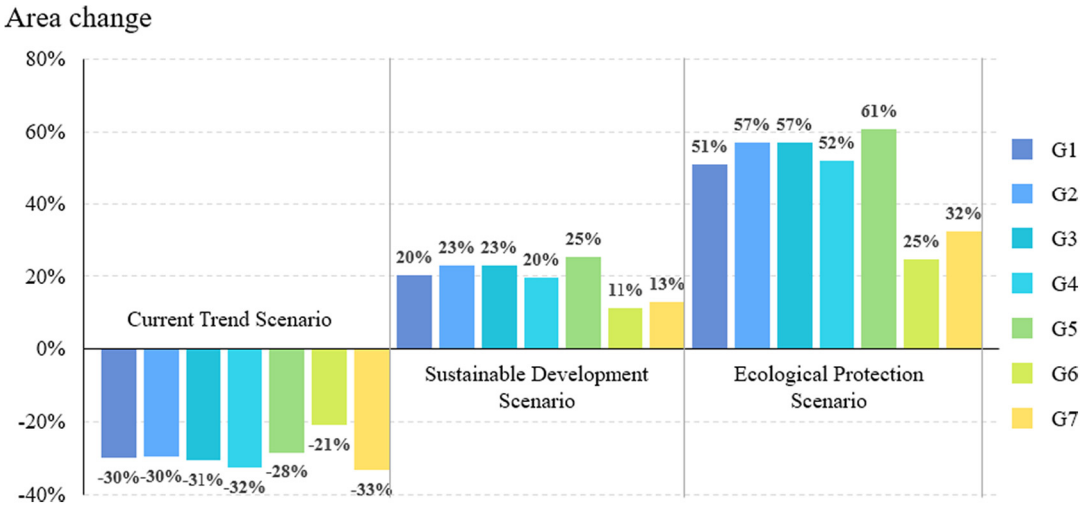

Fig. 8. Change of mangrove potential distribution areas under different land-use scenarios.

mangroves in Hainan Province showed that the aquaculture area increased in 1966–2009, resulting in mangrove fragmentation and reduction (Herbeck et al., 2020). In addition, uncontrolled urban expansion is the most important threat for mangroves in developing countries and regions. Urbanization has destroyed more than 30% of the Brazilian southeast mangrove forests (Moschetto et al., 2020). In Honduras, 19.1% of mangroves have been converted to urban areas since 1985 (Tuholskea et al., 2017). In Guangdong Province, there was a correlation between the increase in urban regions and the loss of mangrove forests, which became more apparent with time (Ai et al., 2020). Furthermore, land-use change not only directly affects the coastal estuarine area, but also disturbs total direct runoff regimes, shifts upstream catchment areas, and affects freshwater inputs to mangroves (Bhattachan et al., 2018; Feng et al., 2020; Mafi-Gholami et al., 2020b).

In this study, land-use changes not only caused suitable habitats for mangroves to be occupied, but also affected the protection of mangroves. Under CTS, mangrove patches not only showed fragmentation, but also tended to retreat seawards because of the expansion of artificial land. Therefore, the construction of mangrove nature reserves faces a dilemma to a certain extent. Although the government planned to increase the protection rate of mangrove habitats by setting or expanding nature reserves, it has been difficult to extend the reserves to artificial land. In Guangdong Province, although the mangrove conservation rate of mangrove nature reserves increased from the 1980s to the 2010s, most mangroves have been isolated by aquaculture ponds and buildings from terrestrial habitats (Peng et al., 2016). Therefore, nature reserves had no choice but to extend their boundaries to low intertidal zones where mangroves were virtually impossible to grow. This reduced the actual protection rate of suitable mangrove habitats after 2000 (Peng et al., 2016). Hence, owing to the influence of land-use patterns, there may even be a loss of mangrove habitat under the virtual increase in nature reserves.

Our results also demonstrated that changes in land-use policies can significantly enhance the potential mangrove survival space. Even if the most radical protection and restoration strategy (EPS) is not adopted, the mangrove habitat degradation trend under SDS could be decreased substantially or even reversed. Therefore, based on scientific demonstration and after the inquiry of stakeholders, feasible land-use policies should be put forward to promote the restoration of mangroves. Possible resistance may come from stakeholders like aquaculture owners. The success rate of coastal fishpond farming in southern China is only about 35%, and 30% of aquaculture ponds are currently abandoned (Paulson Institute, 2020). Thus, it would be possible to return some aquacultural land to wetland, including abandoned aquaculture ponds and some of the ponds that cause the most serious disturbance to mangroves, to minimize the impact on the livelihood of local communities. Appropriate ecological compensation also should be considered in local mangrove conservation and restoration action plans. Moreover, our prediction results indicated that the G6 species were the least sensitive to the improved land-use policies. Thus, further conservation strategies are recommended to maintain and recover this group in addition to land-use policies.

4.3. Study uncertainty and improvement

Previous studies on mangrove distribution used a single SDM to explain the influence of natural environmental factors on current mangrove distribution (Charrua et al., 2020; Hu et al., 2020a), with climate change, storms, and erosion being used as driving factors by several dynamic studies to evaluate past, or predict future, changes in mangrove distribution (Mafi-Gholami et al., 2020a; Cameron et al., 2021; Thakur et al., 2021). However, land use often plays a direct role in the change in mangrove distribution. A study spanning 35 years showed that the zones accessible to human activities are affected by land cover changes significantly more than by natural drivers (Quader et al., 2017). Hu et al. (2020b) overlaid land-use patterns in mangrove-suitable areas to assess the current restoration potential. However, few studies have applied the quantitative prediction of land-use change with the simulation of mangrove distribution change in the future. This study proved that MaxEnt and Dyna-CLUE models can be successfully coupled to find available mangrove habitats under different land-use policies. In addition to statistical verification, the modeled result was compared with the results of a traditional forestry field survey as another kind of model validation. In the current scenario, the maximum potential habitat was estimated to be 34,531 ha, which is close to the 32,326 ha obtained through the forestry surveys (He et al., 2006).

Although the method was effective, some improvements can still be made in future studies. For example, the availability of data limited the operating resolution of the MaxEnt model. The deductive method was used to couple the two models (Bastin et al., 2019; Vessella and Schirone, 2013) because the dataset resolution of the MaxEnt model was 1 km (the best resolution available in the World Bioclimatic Database), whereas the resolution of the land-use data was 250 m. Therefore, the two models had to be trained separately at different resolutions. This may have caused the mangrove habitat extent to be over-estimated because the Maxent model could not identify environmental heterogeneity within 1 km. The use of the deductive method with higher-resolution land use data could constrain the habitat extent and compensate for this shortcoming to some extent. If the resolution of marine environmental data can be improved to match that of LULC data, better model coupling pathways could be adopted. For instance, LULC data could be treated as one of the environmental variables in the MaxEnt model and used directly as input drivers (Wang et al., 2020a).

In this study, land-use patterns were adopted as crucial drivers to predict the future changes of mangrove habitats. However, the actual mangrove distribution can also be affected by other factors. The expansion of mangrove forests takes at least five to seven years due to the afforestation cycle and survival rate (Wodehouse and Rayment, 2019). Long-term survivorship and stable mangrove stands may require more than 10 years (Salmo et al., 2013; Azman et al., 2021). Hence, although the impact of land-use changes on mangrove potential habitats has been clearly revealed, actual changes in mangrove distribution may take a long time to manifest. In addition, this study only focused on the spatial pattern change, whereas mangrove degradation drivers such as pollution, excavation, and cultivation within the mangrove forest were not fully considered.

5. Conclusion

Predicting the spatial extent of mangrove habitats under land-use pressure is one of the main challenges for mangrove restoration planning and management. Mangrove forest distribution is not only related to environmental conditions but is also affected by land development, such as urbanization, cultivation, and aquaculture. Coupling SDM and land-use change models, we proposed an integrated framework to assess spatiotemporal changes in mangrove habitats. The land-use driving effects on different mangrove species were also analyzed and compared based on the MaxEnt model and Dyna-CLUE model in Guangdong, China. Among three land-use scenarios, keeping the policy as CTS will decrease mangrove species by approximately 30%. Meanwhile, mangrove distribution areas could be increased by 11%–61% under SDS and EPS, and the fragmentation of scattered habitat patches could also be improved. Detailed mangrove habitat distribution characteristics can be used to guide habitat restoration practices for each group. For example, species in G6, which were listed as endangered or near-threatened species, had difficulty achieving effective growth even under aggressive protection and restoration land-use scenarios, indicating that additional conservation efforts should be made for these species. The coupled use of MaxEnt and Dyna-CLUE models proved complementary, offering insights into spatially explicit outcomes, and could quantify the impacts of different land-use policies on these outcomes.

Declaration of competing interest

The authors declare that they have no known competing financial interests or personal relationships that could have appeared to influence the work reported in this paper.

Acknowledgments

This work is funded by the National Key Research and Development Program of China (Grant Number 2017YFC0506105, 2019YFE0124700), the National Natural Science Foundation of China (41906127, 42076163), the Provincial Natural Science Foundation of Fujian (2020J05078), and the China-ASEAN Maritime Cooperation fund "Monitoring and conservation of the coastal ecosystem in the South China Sea".

CRediT authorship contribution statement

Yuyu Wang and **Bixiao Chao**, Methodology, Software, Writing, both authors contributed equally to this work, **Peng Dong**: Data curation, Software, **Dian Zhang**: Data curation, Software, **Weiwei Yu**: Investigation, **Wenjia Hu**: Conceptualization, Funding acquisition, Methodology, Software, Writing, **Zhiyuan Ma**: Resources, Investigation, **Guangcheng Chen**: Resources, Investigation, **Zhenghua Liu**: Data curation, **Bin Chen**: Review, Funding acquisition, Supervision.

References

Ai, B., Ma, C.L., Zhao, J., Zhang, R., 2020. The impact of rapid urban expansion on coastal mangroves: a case study in Guangdong Province, China. Front. Earth Sci. 14, 37–49. https://doi.org/10.1007/s11707-019-0768-6.

Alongi, D.M., 2008. Mangrove forests: resilience, protection from tsunamis, and responses to global climate change. Estura. Coast. Shelf. S. 76, 1–13. https://doi.org/10.1016/j.ecss.2007.08.024.

Atkinson, S.C., Jupiter, S.D., Adams, V.M., Ingram, J.C., Narayan, S., Klein, C.J., Possingham, H.P., 2016. Prioritising mangrove ecosystem services results in spatially variable management priorities. PLoS One 11, e0151992. https://doi.org/10.1371/journal.pone.0151992.

Azman, M.S., Sharma, S., Amir, M., Shaharudin, M.A.M., Hamzah, M.L., Adibah, S.N., Zakaria, M., Mackenzie, R., 2021. Stand structure, biomass and dynamics of naturally regenerated and restored mangroves in Malaysia. For. Ecol. Manag. 482. https://doi.org/10.1016/j.foreco.2020.118852.

Bastin, J.F., Finegold, Y., Garcia, C., Mollicone, D., Rezende, M., Routh, D., Zohner, C.M., Crowther, T.W., 2019. The global tree restoration potential. Science 365, 76–79. https://doi.org/10.1126/science.aax0848.

Bhattachan, A., Emanuel, R.E., Ardon, M., Bernhardt, E.S., Anderson, S.M., Stillwagon, M.G., Ury, E.A., BenDor, T.K., Wright, J.P., 2018. Evaluating the effects of land-use change and future climate change on vulnerability of coastal landscapes to saltwater intrusion. Elementa-Sci. Anthrop. 6, 62. https://doi.org/10.1525/elementa.316.

Bittner, R.E., Roesler, E.L., Barnes, M.A., 2020. Using species distribution models to guide seagrass management. Estuar. Coast. Shelf. S. 240, 106790. https://doi.org/10.1016/j.ecss.2020.106790.

Blasco, F., Saenger, P., Janodet, E., 1996. Mangroves as indicators of coastal change. Catena 27, 167–178. https://doi.org/10.1016/0341-8162(96)00013-6.

Cameron, C., Maharaj., A., Kennedy, B., Tuiwawa., S., Goldwater, N., Soapi, K., Lovelock, C.E., 2021. Landcover change in mangroves of Fiji: implications for climate change mitigation and adaptation in the Pacific. Environ. Chall. 2021, 100018. doi:https://doi.org/10.1016/j.envc.2020.100018.

Chakraborty, A., Joshi, P., Sachdeva, K., 2016. Predicting distribution of major forest tree species to potential impacts of climate change in the central Himalayan region. Ecol. Eng. 97, 593–609. https://doi.org/10.1016/j.ecoleng.2016.10.006.

Charrua, A.B., Bandeira, S.O., Catarino, S., Cabral, P., Romeiras, M.M., 2020. Assessment of the vulnerability of coastal mangrove ecosystems in Mozambique. Ocean Coast. Manag. 189, 105145. https://doi.org/10.1016/j.ocecoaman.2020.105145.

Chen, L., Wang, W., Zhang, Y., Lin, G., 2009. Recent progresses in mangrove conservation, restoration and research in China. J. Plant Ecol. 2, 45–54. https://doi.org/10.1093/jpe/rtp009.

Chen, L.J., Wang, W.Q., Zhang, Y.H., Huang, L., Zhao, C.L., Yang, C.S., Yang, Z.W., Chen, Y.C., Xu, H.L., Zhong, C.R., Su, B., Fang, B.Z., Chen, N.M., Zeng, C.Z., Lin, G.H., 2010. Damage to mangroves from extreme cold in early 2008 in southern China. Chin. J. Plant. Ecol. 34, 186–194. https://doi.org/10.3773/j.issn.1005-264x.2010.02.010.

Chen, L.E., Xu, H.M., Xu, H.L., Lin, S.S., Liao, W.B., Xin, G.R., Zan, Q.J., 2012. Investigation of cold damage and renew of several dominant mangrove plants in Neilingding-futian National Nature Reserve of Guangdong Province, China. Guangdong For. Sci. Technol. 28, 37–41.

Chen, L.Z., Zheng, W.J., Yang, S.C., Wang, W.Q., Zhang, Y.H., 2017. Research progresses of mangrove cold-tolerant classes and seral classes, and their responses to climate change. J. Xiamen Univ. Nat. Sci. 56, 305–313. https://doi.org/10.6043/j.issn.0438-0479.201612004.

Dan, X.Q., Liao, B.W., Wu, Z.B., Wu, H.J., Bao, D.M., Dan, W.Y., Liu, S.H., 2016. Resources, conservation status and main threats of mangrove wetlands in China. Ecol. Environ. Sci. 25, 1237–1243. https://doi.org/10.16258/j.cnki.1674-5906.2016.07.021.

Fan, H.Q., Wang, W.Q., 2017. Some thematic issues for mangrove conservation in China. J. Xiamen Univ. 56, 323–330. https://doi.org/10.6043/j.issn.0438-0479.201612003.

FAO, 2007. The World's Mangroves 1980-2005. Food and Agriculture Organization of the United Nations, Rome http://www.fao.org/3/a1427e/a1427e00.htm.

Feng, Z., Tan, G., Xia, J., Shu, C., Chen, P., Wu, M., Wu, X., 2020. Dynamics of mangrove forests in Shenzhen Bay in response to natural and anthropogenic factors from 1988 to 2017. J. Hydrol. 591, 125271. https://doi.org/10.1016/j.jhydrol.2020.125271.

Gevana, D., Camacho, L., Carandang, A., Sofronio, C., Sang, J., 2015. Land use characterization and change detection of a small mangrove area in Banacon Island, Bohol, Philippines using a maximum likelihood classification method. For. Sci. Technol. 11, 197–205. https://doi.org/10.1080/21580103.2014.996611.

Giri, C., Ochieng, E., Tieszen, L.L., Zhu, Z., Singh, A., Loveland, T., Masek, J., Duke, N., 2011. Status and distribution of mangrove forests of the world using earth observation satellite data. Glob. Ecol. Biogeogr. 20, 154–159. https://doi.org/10.1111/j.1466-8238.2010.00584.x.

Gong, J., Hu, Z., Chen, W., Liu, Y., Wang, J., 2018. Urban expansion dynamics and modes in metropolitan Guangzhou, China. Land Use Policy 72, 100–109. https://doi.org/10.1016/j.landusepol.2017.12.025.

He, K.J., Lin, S.M., Lin, Z.D., 2006. Mangrove resource and its strategy of conservation and management in Guangdong Province. Forest. Environ. Sci. 22, 89–93. https://doi.org/10.3969/j.issn.1006-4427.2006.02.022.

Herbeck, L.S., Krumme, U., Andersen, T.J., Jennerjahn, T.C., 2020. Decadal trends in mangrove and pond aquaculture cover on Hainan (China) since 1966: mangrove loss, fragmentation and associated biogeochemical changes. Estuar. Coast. Shelf. S. 233, 106531. https://doi.org/10.1016/j.ecss.2019.106531.

Hu, W.J., Wang, Y.Y., Dong, P., Zhang, D., Yu, W.W., Ma, Z.Y., Chen, G.C., Liu, Z.H., Du, J.G., Chen, B., Lei, G., 2020a. Predicting potential mangrove distributions at the global northern distribution margin using an ecological niche model: determining conservation and reforestation involvement. For. Ecol. Manag. 478, 118517. https://doi.org/10.1016/j.foreco.2020.118517.

Hu, W.J., Wang, Y.Y., Zhang, D., Yu, W.W., Chen, G.C., Xie, T., Liu, Z.H., Ma, Z.Y., Du, J.G., Chao, B.X., Lei, G.C., Chen, B., 2020b. Mapping the potential of mangrove forest restoration based on species distribution models: a case study in China. Sci. Total Environ. 748, 142321. https://doi.org/10.1016/j.scitotenv.2020.142321.

Huang, L.Y., Shi, X.F., Mo, Z.C., Yan, B., Pan, L.H., 2020. Distribution and population characteristics of the rare and endangered exclusive mangrove plant *Acanthus ebracteatus* in Guangxi. J. Guangxi Acad. Sci. 36, 1–8. https://doi.org/10.13656/j.cnki.gxkx.20201023.001.

Jayasinghe, S.L., Kumara, L., 2019. Modeling the climate suitability of tea [*Camellia sinensis* (L.) O. Kuntze] in Sri Lanka in response to current and future climate change scenarios. Agric. For. Meteorol. 272-273, 10–117. https://doi.org/10.1016/j.agrformet.2019.03.025.

Jia, M., Wang, Z., Zhang, Y., Mao, D., Wang, C., 2018. Monitoring loss and recovery of mangrove forests during 42 years: the achievements of mangrove conservation in China. Int. J. Appl. Earth. Obs. 73, 535–545. https://doi.org/10.1016/j.jag.2018.07.025.

Johnson, C.J., Nielsen, S.E., Merrill, E.H., McDonald, T.L., B.M, S., 2006. Resource selection functions based on use-availability data: theoretical motivation and evaluation methods. J. Wildl. Manag. 70, 347–357. https://doi.org/10.2193/0022-541X(2006)70[347:RSFBOU]2.0.CO;2.

Kulhanek, S.A., Leung, B., Ricciardi, A., 2011. Using ecological niche models to predict the abundance and impact of invasive species: application to the common carp. Ecol. Appl. 21, 203–213. https://doi.org/10.1890/09-1639.1.

Li, X., Mao, F., Du, H., Zhou, G., Xing, L., Liu, T., Han, N., Liu, Y., Zhu, D., Zheng, J., Dong, L., Zhang, M., 2019. Spatiotemporal evolution and impacts of climate change on bamboo distribution in China. J. Environ. Manag. 248, 109265. https://doi.org/10.1016/j.ecolind.2019.105572.

Li, H.Y., Peng, Y.S., Liu, J.J., Wang, S.G., Chen, G.Z., 2016. Current state of mangrove floristic composition and characteristics of communities on the eastern coast of Guangdong Province. Acta Ecol. Sin. 36, 252–260. https://doi.org/10.5846/stxb201408031548.

Liao, J., Shao, G., Wang, C., Tang, L., Huang, Q., Qiu, Q., 2019. Urban sprawl scenario simulations based on cellular automata and ordered weighted averaging ecological constraints. Ecol. Indic. 107, 105572. https://doi.org/10.1016/j.ecolind.2019.105572.

Liao, B., Zhang, Q., 2014. Distribution and species composition of mangroves in China. Wetland Sci. 12, 435–440. https://doi.org/10.13248/j.cnki.wetlandsci.2014.04.005.

Lin, P., Fu, Q., 1995. Environmental Ecology and Economic Utilization of Mangrove in China. Higher Education Press, Beijing.

Lin, K., Zhang, Q., Jian, S., Wang, R., Shen, W., Lu, H., Ren, H., Xu, F., 2006. Mangrove resource and sustainable development at Zhanjiang. Ecol. Sci. 25, 222–225. https://doi.org/10.3969/j.issn.1008-8873.2006.03.008.

Lv, L., Luo, H., Zhang, B., 2012. Relationship between electricity consumption and economic growth of Guangdong Province in China. Front. Energy Res. 6, 351–355. https://doi.org/10.1007/s11708-012-0209-7.

Mafi-Gholami, D., Jaafari, A., Zenner, E.K., Kamari, A.N., Bui, D.T., 2020a. Spatial modeling of exposure of mangrove ecosystems to multiple environmental hazards. Sci. Total Environ. 740, 140167. https://doi.org/10.1016/j.scitotenv.2020.140167.

Mafi-Gholami, D., Zenner, E.K., Jaafari, A., Bui, D.T., 2020b. Spatially explicit predictions of changes in the extent of mangroves of Iran at the end of the 21st century. Estuar. Coast. Shelf. S. 237, 106644. https://doi.org/10.1016/j.ecss.2020.106644.

Malik, A., Mertz, O., Fensholt, R., 2017. Mangrove forest decline: consequences for livelihoods and environment in South Sulawesi. Reg. Environ. Chang. 17, 157–169. https://doi.org/10.1007/s10113-016-0989-0.

Mao, L.J., 2011. Assessment of Changes in Mangrove Forest Patterns from Multitemporal Remotely Sensed Imagery over Zhanjiang City, Guangdong Province. Master Thesis. Nanjing Forestry University.
MNR, NFGA, 2020. Special action plan for mangrove protection and restoration (2020-2025). http://www.gov.cn/xinwen/2020-08/30/content_5538506.htm (accessed on 24 November 2020).
Moschetto, F.A., Ribeiro, R.B., De Freitasa, D.M., 2020. Urban expansion, regeneration and socioenvironmental vulnerability in a mangrove ecosystem at the southeast coastal of São Paulo, Brazil. Ocean Coast. Manag. 24, 105418. https://doi.org/10.1016/j.ocecoaman.2020.105418.
NBSC, 2020. 2020 China Statistical Yearbook. China Statistics Press, Beijing http://www.stats.gov.cn/tjsj/ndsj/2020/indexch.htm.
Overmars, K.P., Verburg, P.H., Veldkamp, T., 2007. Comparison of a deductive and an inductive approach to specify land suitability in a spatially explicit land use model. Land Use Policy 24, 584–599. https://doi.org/10.1016/j.landusepol.2005.09.008.
Paulson Institute, 2020. Research report on mangrove protection and restoration strategy in China. https://paulsoninstitute.org.cn/wp-content/uploads/2020/06/%E4%B8%AD%E5%9B%BD%E7%BA%A2%E6%A0%91%E6%9E%97%E4%BF%9D%E6%8A%A4%E4%B8%8E%E6%81%A2%E5%A4%8D%E6%88%98%E7%95%A5%E7%A0%94%E7%A9%B6%E6%8A%A5%E5%91%8A%E2%80%94%E6%91%98%E8%A6%81%E7%89%88.pdf (accessed on 22 October 2020).
Peng, Y.S., Li, H.Y., Zeng, Y., Peng, S.H., Xiao, H., 2015. Current status and site conditions of mangrove forest community in Hanjiang River Delta of Guangdong Province. Sci. Silvae Sin. 51, 103–112. https://doi.org/10.11707/j.1001-7488.20151213.
Peng, Y., Zheng, M., Zheng, Z., Wu, G., Chen, Y., Xu, H., Tian, G., Peng, S., Chen, G., Lee, S.Y., 2016. Virtual increase or latent loss? A reassessment of mangrove populations and their conservation in Guangdong, southern China. Mar. Pollut. Bull. 109, 691–699. https://doi.org/10.1016/j.marpolbul.2016.06.083.
Peng, K., Jiang, W., Deng, Y., Liu, Y., Wu, Z., Chen, Z., 2020. Simulating wetland changes under different scenarios based on integrating the random forest and CLUE-S models: a case study of Wuhan urban agglomeration. Ecol. Indic. 117, 106671. https://doi.org/10.1016/j.ecolind.2020.106671.
Phillips, S.J., Anderson, R.P., Schapire, R.E., 2006. Maximum entropy modeling of species geographic distributions. Ecol. Model. 190, 231–259. https://doi.org/10.1016/j.ecolmodel.2005.03.026.
Phillips, S.J., Anderson, R.P., Dudik, M., Schapire, R.E., Blair, M.E., 2017. Opening the black box: an open-source release of MaxEnt. Ecography 40, 887–893. https://doi.org/10.1111/ecog.03049.
Pontius, R.G.J., Boersma, W., Castella, J.C., Clarke, K., Nijs, T.D., Dietzel, C., Duan, Z., 2008. Comparing the input, output, and validation maps for several models of land change. Ann. Reg. Sci. 42, 11–37. https://doi.org/10.1007/s00168-007-0138-2.
Quader, M.A., Agrawal, S., Kervyn, M., 2017. Multi-decadal land cover evolution in the Sundarban, the largest mangrove forest in the world. Ocean Coast. Manag. 139, 113–124. https://doi.org/10.1016/j.ocecoaman.2017.02.008.
Quisthoudt, K., Schmitz, N., Randin, C.F., Dahdouh-Guebas, F., Robert, E.M.R., Koedam, N., 2012. Temperature variation among mangrove latitudinal range limits worldwide. Trees-Struct. Funct. 26, 1919–1931. https://doi.org/10.1007/s00468-012-0760-1.
Richards, D.R., Friess, D.A., 2016. Rates and drivers of mangrove deforestation in Southeast Asia. Proc. Natl. Acad. Sci. U.S.A. 113, 344–349. https://doi.org/10.1073/pnas.1510272113.
Sakayarote, K., Shrestha, R.P., 2019. Simulating land use for protecting food crop areas in northeast Thailand using gis and dyna-clue. J. Geogr. Sci. 29, 803–817. https://doi.org/10.1007/s11442-019-1629-7.
Salmo, S.G., Lovelock, C., Duke, N.C., 2013. Vegetation and soil characteristics as indicators of restoration trajectories in restored mangroves. Hydrobiologia 720, 1–18. https://doi.org/10.1007/s10750-013-1617-3.
Sardar, P., Samadder, S.R., 2021. Understanding the dynamics of landscape of greater Sundarban area using multi-layer perceptron Markov chain and landscape statistics approach. Ecol. Indic. 121, 106914. https://doi.org/10.1016/j.ecolind.2020.106914.
Sasmito, S.D., Taillardat, P., Clendenning, J.N., Cameron, C., Friess, D.A., Murdiyarso, D., Hutley, L.B., 2019. Effect of land-use and land-cover change on mangrove blue carbon: a systematic review. Glob. Chang. Biol. 25, 4291–4302. https://doi.org/10.1111/gcb.14774.
Sillanpaa, M., Vantellingen, J., Friess, D.A., 2017. Vegetation regeneration in a sustainably harvested mangrove forest in West Papua, Indonesia. For. Ecol. Manag. 390, 137–146. https://doi.org/10.1016/j.foreco.2017.01.022.
Spalding, M.D., Kainuma, M., Collins, L., 2010. World Atlas of Mangroves. Earthscan, London.
Swets, J.A., 1988. Measuring the accuracy of diagnostic systems. Science 240, 1285–1293. https://doi.org/10.1126/science.3287615.
Tesfaw, A.T., Pfaff, A., Kroner, R.E.G., Qin, S.Y., Medeiros, R., Mascia, M.B., 2018. Land-use and land-cover change shape the sustainability and impacts of protected areas. Proc. Natl. Acad. Sci. U.S.A. 115, 2084–2089. https://doi.org/10.1073/pnas.1716462115.
Thakur, S., Mondal, I., Bar, S., Nandi, S., Ghosh, P.B., Das, P., De, T.K., 2021. Shoreline changes and its impact on the mangrove ecosystems of some islands of Indian Sundarbans, North-East coast of India. J. Clean. Prod. 284, 124764. https://doi.org/10.1016/j.jclepro.2020.124764.
Thomas, N., Lucas, R., Bunting, P., Hardy, A., Rosenqvist, A., Simard, M., 2017. Distribution and drivers of global mangrove forest change, 1996–2010. PLoS One 12, e0179302. https://doi.org/10.1371/journal.pone.0179302.
Trisurat, Y., Alkemade, R., Verburg, P.H., 2010. Projecting land-use change and its consequences for biodiversity in northern Thailand. Environ. Manag. 45, 626–639. https://doi.org/10.1007/s00267-010-9438-x.
Tuholskea, C., Tane, Z., López-Carra, D., Roberts, D., Cassels, S., 2017. Thirty years of land use/cover change in the Caribbean: assessing the relationship between urbanization and mangrove loss in Roatán, Honduras. Appl. Geogr. 88, 84–93. https://doi.org/10.1016/j.apgeog.2017.08.018.
Valiela, I., Bowen, J.L., York, J.K., 2001. Mangrove forests: one of the world's threatened major tropical environments. Bioscience 51, 807–815. https://doi.org/10.1641/0006-3568(2001)051[0807:MFOOTW]2.0.CO;2.
Verburg, P.H., Overmars, K.P., 2009. Combining top-down and bottom-up dynamics in land use modeling: exploring the future of abandoned farmlands in Europe with the Dyna-CLUE model. Landsc. Ecol. 24, 1167–1181. https://doi.org/10.1007/s10980-009-9355-7.
Verburg, P.H., Soepboer, W., Veldkamp, A., Limpiada, R., Espaldon, V., Mastura, S.S.A., 2002. Modeling the spatial dynamics of regional land use: the CLUE-S model. Environ. Manag. 30, 391–405. https://doi.org/10.1007/s00267-002-2630-x.
Vessella, F., Schirone, B., 2013. Predicting potential distribution of *Quercus suber* in Italy based on ecological niche models: conservation insights and reforestation involvements. For. Ecol. Manag. 304, 150–161. https://doi.org/10.1016/j.foreco.2013.05.006.
Wang, G., Wang, C., Guo, Z.R., Dai, L.J., Wu, Y.Q., Liu, H.Y., Li, Y.F., Chen, H., Zhang, Y.N., Zhao, Y.X., Cheng, H., Ma, T.W., Xue, F., 2020a. Integrating MaxEnt model and landscape ecology theory for studying spatiotemporal dynamics of habitat: suggestions for conservation of endangered red -crowned crane. Ecol. Indic. 116, 106472. https://doi.org/10.1016/j.ecolind.2020.106472.
Wang, W.Q., Fu, H.F., Lee, S.Y., Fan, H.Q., Wang, M., 2020b. Can strict protection stop the decline of mangrove ecosystems in China? From rapid destruction to rampant degradation. Forests 11, 55. https://doi.org/10.3390/f11010055.
Wei, B., Wang, R., Hou, K., Wang, X., Wu, W., 2018. Predicting the current and future cultivation regions of Carthamus tinctorius L. using MaxEnt model under climate change in China. Glob. Ecol. Conserv. 16, e00477. https://doi.org/10.1016/j.gecco.2018.e00477.
Wischmeier, W.H., Smith, D.D., 1978. Predicting rainfall erosion losses: a guide for conservation planning. Agriculture Handbook No. 537 , pp. 285–291. https://www.mendeley.com/catalogue/0bd77bfe-29ff-3eeb-ab43-a3ccddc4e9f9/.
Wodehouse, D.C.J., Rayment, M.B., 2019. Mangrove area and propagule number planting targets produce sub-optimal rehabilitation and afforestation outcomes. Estuar. Coast. Shelf. S. 222, 91–102. https://doi.org/10.1016/j.ecss.2019.04.003.
Worthington, T., Spalding, M., 2018. Mangrove Restoration Potential: A Global Map Highlighting a Critical Opportunity. https://doi.org/10.17863/CAM.39153 (accessed on 24 November 2020).
Wu, P., Ma, Y., Li, X., Yu, G., 2011. Remote sensing monitoring of the mangrove forests resources of Guangdong Province. J. Mar. Sci. 29, 16–24.
Wu, Y., Ricklefs, R.E., Huang, Z., Zan, Q., Yu, S., 2018. Winter temperature structures mangrove species distributions and assemblage composition in China. Glob. Ecol. Biogeogr. 27, 1492–1506. https://doi.org/10.1111/geb.12826.
Yang, J.Z., Hu, Y.H., Luo, Y., Xue, C.Q., 2018. Study on the distribution and dynamic change of mangrove in Guangdong. For. Environ. Sci. 34, 24–27.
Zhang, Y., Ding, Y., Wang, W., Li, Y., Wang, M., 2019. Distribution of fish among *Avicennia* and *Sonneratia* microhabitats in a tropical mangrove ecosystem in south China. Ecosphere 10, e02759. https://doi.org/10.1002/ecs2.2759.